Damage and cracking in thin mud layers



2000 J. Phys. A: Math. Gen. 33 8013

(http://iopscience.iop.org/0305-4470/33/45/301)

J. Phys. A: Math. Gen. **33** (2000) 8013–8028. Printed in the UK PII: S0305-4470(00)12631-9

# Damage and cracking in thin mud layers

Raffaele Cafiero†, Guido Caldarelli‡ and Andrea Gabrielli§

† PMMH Ecole Sup. de Physique et de Chimie Industrielles (ESPCI), 10, rue Vauquelin, 75231 Paris Cedex 05, France

‡ INFM Sezione di Roma1, Dipartimento di Fisica, Università di Roma 'La Sapienza', P. le A Moro 2, I-00185 Roma, Italy

§ Laboratoire de Physique de la Matière Condensée, Ecole Polytechnique, 91128 Palaiseau Cedex, France

Received 9 March 2000, in final form 11 September 2000

**Abstract.** We present a detailed study of a two-dimensional lattice model introduced to describe mud cracking in the limit of extremely thin layers. In this model to each bond in the lattice is assigned a (quenched) random breaking threshold. Fractures proceed by selecting the 'weakest' part of the material (i.e. the smallest value of the threshold). A local damage rule is also implemented, by using two different types of weakening of the neighbouring sites, corresponding to different physical situations. We present the results of numerical simulations on this model. We also derive some analytical results through a probabilistic approach known as run time statistics. In particular, we find that the total time to divide the sample scales with the square power $L^2$ of the linear size $L$ of the lattice. This result is not straightforward since the percolating cluster has a non-trivial fractal dimension. Furthermore, we present here a formula for the mean weakening of the whole sample during the evolution.

## 1. Introduction

In recent years, many models have been proposed to describe the formation of cracks in different kinds of material. These models are usually based either on on-lattice cellular automata or on continuous equations [1–3].

In this paper we present a careful and detailed study of a minimal fracture model that has been introduced in order to describe the main features of paint desiccation-like phenomena [4]. The purpose of this paper is to focus on the statistical properties of these phenomena on the basis of recent experimental findings [5]. Following the results of [5], we assumed that the main source of stress is given by the *local* friction between the layer of material and the bottom surface of the container. Moreover, it has been noticed that the characteristic size of crack patterns varies linearly with the layer thickness. In the limit of zero thickness *crack patterns lose their polygonal structure* (the characteristic size of the polygons is zero) and become *branched fractals*.

In order to model this behaviour, we present here a very simple lattice model (introduced in [4]), inspired by invasion percolation (IP) [6] and by the vectorial and scalar models described in [7, 8]. Here, we present an extended report of the property of the model, together with a detailed description of the analytical calculations, as well as new numerical and theoretical results.

Most of the cellular automata models for *quasi-static* fractures, describe crack evolution through a non-local Laplacian field (i.e. electric field) acting on a solid network of bonds or

0305-4470/00/458013+16$30.00  

sites [8]. In some of them the stress field step by step is computed by minimizing the energy of the system during the evolution. In such a case one deals with vectorial equations whose components are similar to the equations describing the action of a Laplacian field [7].

In the model presented instead, no explicit field is present. The effect of the stress is played by an extremal breaking rule and by the damage of the *local* random breaking thresholds. Indeed the damage rule introduces a correlation in the system that drives the evolution through the nearest neighbour bonds of the bond just removed. According to the kind of fracture we deal with, one can introduce different types of damage. In this paper two limiting cases are studied. This model is inspired by the above cited experimental observations [5] that, in an extremely thin layer of mud or paint, the only source of stress is the *local* friction with the container. Moreover, since the drying mud is a mixture of a liquid and a solid (usually amorphous) phase, no long-range stress relaxation is present, although the growing crack can affect the properties of the medium in its neighbourhood. Some important physical properties of the model are explained by using an approach based on the run time statistics (RTS) scheme [9]. In particular, we are able to compute some relevant quantities, such as the evolution of the breaking probability, and of the probability distribution of breaking thresholds.

The paper is organized as follows. In section 2 the model is described. In section 3 the results of numerical simulations are presented. In section 4 the model is studied analytically, and theoretical and numerical results are compared.

## 2. The model

We considered a square lattice where a random variable $x_i$ is assigned to each bond $i$. The $x_i$ are independently extracted from an uniformly distributed probability density defined between 0 and 1. At each time-step $t$, the bond with the smallest value of the variable is broken (removed). Then damage (weakening) is applied, by reducing the value of $x$ for the nearest neighbour bonds. This evolution is repeated until a connected, percolating, subset (infinite cluster) of removed bonds appears, dividing the system into two disconnected parts.

In the following, we will indicate the set of broken bonds up to time $t$ by $C_t$, and the set of non-broken bonds by $\partial C_t$. The number of bonds belonging to $C_t$ is $\|C_t\| = t$, while $\|\partial C_t\| = N - t$ (where $N$ is the total number of bonds in the lattice), in fact $\partial C_t$ is composed by the whole lattice without the bonds in $C_t$. Two different types of weakening are actually applied: either by direct weakening or by re-distribution of the stress. In the first case (rule 1), the nearest neighbours of the removed bonds are weakened, by extracting a new threshold $x_i'$ for them between 0 and the former value $x_i$ (in this case an average weakening of one half of the former value at time is obtained). In the second case (rule 2), each nearest neighbour has a threshold weakened by a fraction of the threshold of the bond just removed. Both cases mimic the damage produced by the enhancement of the stress nearby crack tips. The first case refers to a situation where stochasticity (thermal fluctuations) is important in the determination of the new thresholds [1]. The second case refers to a situation where the disorder distribution around the tip plays the leading role. As regards the real case of mud cracking, the two-dimensional lattice is supposed to describe a very thin layer of mud (or paint), and the quenched disorder *accounts for local stress induced by inhomogeneous desiccation of the sample*. Since the evolution of cracks in mud desiccation is assumed to be a slow process, the dynamics is assumed to be *quasi-static*, i.e. one microscopical break with relative damage for each time-step. Some authors correctly point out that otherwise time-dependent effects and a non-equilibrium dynamics are relevant in crack propagation [10].

In this model the external field (applied stress) and the response of the material (strain of bonds) have been eliminated. The only relevant quantity is the breaking threshold for

**Table 1.** Fractal dimension of the spanning cluster for different sizes and for the two damage rules.

| | $L = 64$ | $L = 128$ | $L = 256$ |
|---|---|---|---|
| $D_f$ (damage rule 1) | 1.75(2) | 1.74(2) | 1.74(2) |
| $D_f$ (damage rule 2) | 1.73(2) | 1.75(2) | 1.76(2) |

the bonds, whose dynamics is suitably chosen to reproduce the evolution of cracks. This threshold simulates the presence of a local stress field, acting directly on each bond. Our assumption is based on the experimental results in [5], where, as the mud layer becomes thinner, only the inhomogeneities drive the nucleation of cracks. Furthermore, the hypothesis of crack development under the same state of strain is usually applied in the presence of thermal gradients [11]. Furthermore it is also commonly reported in experiments of loading of softened material [12–14]. Hence, such a model is particularly suitable to describe, for example, paint drying, where the stress applied to the painted surface depends on the local action of external conditions (density gradient in the paint). Moreover, its simplicity allows us to study analytically the properties of the model and to compute some quantity of interest, such as the mean resistance of the sample.

## 3. Numerical results

Numerical simulations, with cylindrical symmetry (periodic boundary conditions in the horizontal direction), for various system sizes $L$ have been performed. The dynamics stops as soon as a crack spanning the system in the vertical direction appears. Both damage rules are implemented, and they are both discussed. Despite the simplicity of the dynamical rules, the results are rather interesting. We have computed the fractal dimension of the percolating cluster, the distribution of the size of clusters of broken bonds, the avalanche size distribution (in order to check whether long-range temporal correlations are present) and the probability distribution of the breaking thresholds at the percolation time. An avalanche can be defined as an ensemble of causally and geometrically connected breakdowns (see below for a rigorous definition). Under this respect the size distribution of such avalanches represents the probability of a large or small response of the system to an external solicitation. For example a power-law distribution represents a critical state of the system where the response does not show any characteristic size.

The fractal dimension $D_f$ of the percolating cluster is computed using the box-counting method. The analysis is restricted to the spanning cluster to reduce the finite-size effects present in the smaller clusters. The results of the box-counting analysis are reported in table 1 for the different sizes and for the two damage rules. The values of $D_f$ for the two damage rules coincide within the error bars.

The connected clusters of broken bonds are identified with a standard cluster counting procedure, based on the Hoshen–Kopelman algorithm [15]. Also the distribution of finite clusters is nontrivial, showing a clear power law with exponent $\tau_c = 1.54(2)$ (see figure 1($a$)) for rule 1 and $\tau_c = 1.57(3)$ for rule 2. The plots labelled with ($b$) in figure 1 refer to the avalanche size distribution. This quantity is interesting with respect to recent experiments [16] and models [7, 8] where a power law behaviour of the acoustic emission has been related to self-organized criticality (SOC) [17]. The presence of a SOC-like behaviour would mean that the dynamics of fractures itself leads the sample to a steady state where small variation of the external field can trigger reaction at any length-scale. In particular the external field

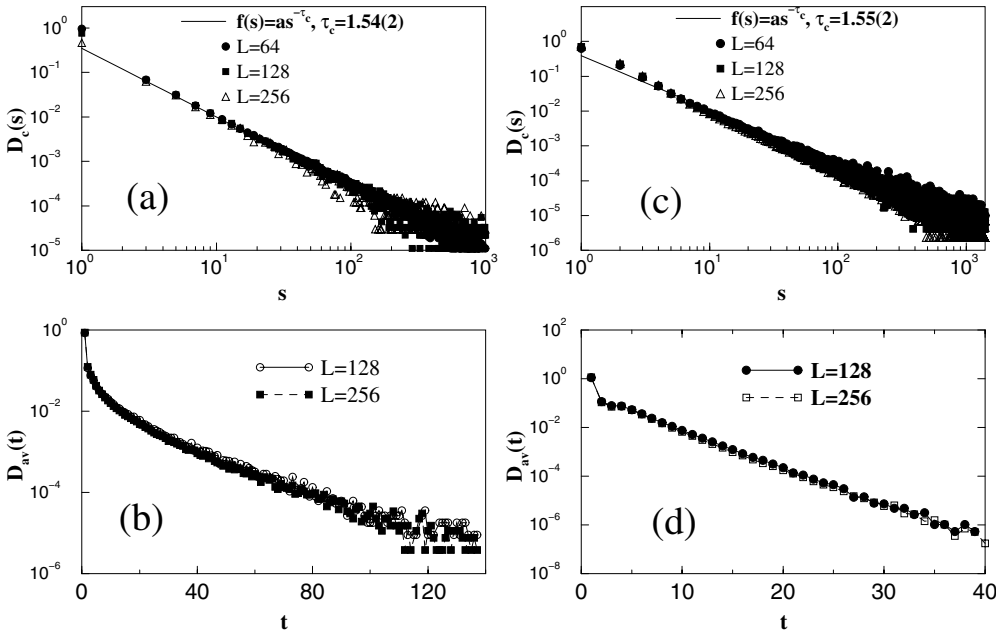


**Figure 1.** (*a*) Probability distribution ($\log_{10}$–$\log_{10}$ plot) $D_c(s)$ of the cluster size, for $L = 64, 128, 256$. (*b*) Avalanche size distribution (linear–$\log_{10}$ plot) $D_{av}(t)$ for $L = 128, 256$. (*c*) and (*d*) The same quantities for the weakening rule 2.

in this case is the applied stress, and the response of the sample can be considered as the energy released (acoustic emission) by one avalanche of cracks, where avalanche means a causally and geometrically connected series of breakdowns. In this oversimplified model the external stress can be considered constant, since the only change after any single breakdown is due the damaging of the nearest neighbours. Consequently, in this paper the size of an avalanche is monitored as a measure for the acoustic emission. An avalanche can be defined as follows. Let us suppose that a bond $i$ grows (i.e. it is broken) at time $t$; this is the *initiator* of an avalanche, which is defined as the set of events geometrically and causally connected to the initial one (bond $i$). 'Causal' connection refers to the weakening following any bond breaking. In particular, when bond $i$ grows at time $t$, the avalanche goes on at time $t + 1$ if a unbroken first-neighbour bond $j$ of $i$ is removed. At time $t + 2$ the avalanche goes on if a bond $k$ grows where $k$ is a unbroken first neighbour of $i$ or $j$. A linear–log plot of the probability distribution of avalanche size, versus sample size $L$, is shown in figure 1(*b*). After a power law transient, an exponential distribution is reached, indicating that a characteristic size exists for the avalanches. One can note that for weakening rule 1 and weakening rule 2 simulations give qualitatively similar results, although for rule 2 the characteristic time of avalanches is smaller. This is easily explained, since the damage rule 2 is less strong than rule 1 and, consequently, the causal connection between subsequent breaking events is weaker.

This result for avalanches is similar to those obtained for a scalar model of dielectric breakdown, but differs from the avalanche behaviour in models of fracture [7, 8]. The explanation of this behaviour is motivated by two arguments. Firstly, in the present definition of an avalanche the threshold is changed only for the nearest neighbours. This introduces a typical length scale, while other definitions consider as the threshold the ratio between local field and resistivity, thus giving the possibility of large-scale correlations. Secondly, in this

model broken bonds *are removed from the system*. This represents a substantial difference from many SOC models with quenched disorder presented in the literature. For example, in a simple toy model of SOC due to Bak and Sneppen [18] (where a similar refresh of thresholds is present) the dynamics produces clear power laws in the avalanche distribution. There, each site (species) deleted is replaced by a new one and is not definitively removed. In our model, instead, the number of candidates $\partial C_t$ to be broken at each time-step decreases in time. This is a crucial point, since indeed power law behaviour in the presence of a scalar field seems to be related to a 'reconstructing rule' that allows one to deal with a system where removed bonds are replaced by new ones. Therefore, only in the case of plastic deformation, one is in the presence of a steady state, as correctly pointed out by [8].

To summarize the content of this section, the fractal dimension, the cluster size distribution and, to some extent, the avalanche size distribution seem to be universal with respect to the two different local damage rules. In the next section the study will focus on some quantities which, instead, are not universal and reproduce the evolution of the mechanical properties of the material during the fracturing dynamics. These quantities are the average probability density of breaking thresholds, or histogram, $\phi_t(x)$, and as a by-product the mean breaking threshold $\langle x \rangle(t)$, which expresses the average resistance to breaking, or rigidity, of the system at time $t$. These quantities will be studied both numerically, and analytically, by using a probabilistic tool called RTS [9].

## 4. RTS derivation of the average weakening of the material

As seen above, the evolution of the crack is described by a quasi-static extremal dynamics in a medium with quenched disorder. The most important question for a theoretical comprehension of the model is: which is the source of the spatio-temporal correlations developed by the dynamics? As pointed in [9] in relation to IP, the source can be found in the memory effects developed by the evolution of the dynamics itself via an interplay between dynamical rules and quenched disorder.

This can be simply realized observing that the knowledge of the growth history up to a time $t$, provides information about the probability distribution and the correlations of the random bond thresholds. This information has to be added to the original information that the thresholds are independently extracted from the uniform probability density in the interval [0, 1]. Moreover this information influences the probabilities of the different possible continuations of the dynamics for larger time. This memory effect can be studied using carefully the notion of conditional probability. This kind of approach to growth dynamics with quenched disorder has been developed in [9, 19], with particular reference to IP. This peculiar probabilistic algorithm is called RTS. A particular modification of this tool is presented here taking into account the damage mechanism, which is not present in IP-like models. Finally, RTS is used in order to predict analytically some relevant quantities such as the evolution of both the average probability density of breaking thresholds of unbroken bonds and of the mean resistance to breakdown $x(t)$ of the material.

Here we provide directly the final RTS formulas together with a brief sketch of their meaning. A detailed derivation of the analytical results of this section is given in the appendix. The RTS approach permits us mainly to answer the following two questions, once given a certain time-ordered geometrical path followed by the dynamics up to time $t$:

(1) what is the *effective* probability density function of the variables $x_i$ of the lattice conditioned to the knowledge of this fixed past dynamical history? and
(2) what is the conditional probability of any further growth event at the next time-step?

In order to introduce operative formulas, let us assume we know the 'one-bond' effective probability density functions $p_{i,t}(x)$ (conditioned to the past dynamical history) for each non-broken bond $i$. As clarified in the appendix, this 'one-bond' formulation of RTS is an approximation of the rigorous one. However, as shown in [20], it is a good approximation when the number of random numbers is large (as in this case).

First of all one can write [9] the breaking probability $\mu_{i,t}$ for each bond $i$ at that time-step:

$$\mu_{i,t} = \int_0^1 \mathrm{d}x\; p_{i,t}(x)\left[\prod_{k(\neq i)}^{\partial C_t}\int_x^1 \mathrm{d}y\; p_{k,t}(y)\right] \tag{1}$$

where $\partial C_t$ is the whole set of unbroken bonds. Note that at time $t$ the number of bonds in $\partial C_t$ is $(2L^2 - t)$, i.e. the total number $2L^2$ of bonds in a square lattice of side $L$ minus the number of broken bonds before time $t$. Equation (1) expresses nothing other than the effective probability that $x_i$ is the minimum in the set $\partial C_t$ conditioned to the past history. The next important step is to update each $p_{j,t}(x)$ by conditioning them to this latest growth event. In this way one obtains the $p_{j,t+1}(x)$s conditioned to the history up to the time-step $t + 1$. The effective probability density at time $t + 1$ of the latest grown bond $i$ is usually called $m_{i,t+1}(x)$, in order to distinguish it from the densities of still unbroken bonds. It is given by

$$m_{i,t+1}(x) = \frac{1}{\mu_{i,t}} p_{i,t}(x)\left[\prod_{k(\neq i)}^{\partial C_t}\int_x^1 \mathrm{d}y\; p_{k,t}(y)\right]. \tag{2}$$

Equation (2) (multiplied by $\mathrm{d}x$) gives the 'effective' probability that $x \leqslant x_i \leqslant x + \mathrm{d}x$, conditioned to the past fixed dynamical history (time-ordered path) up to time $t + 1$: the 'memory' of the history up to time $t$ is 'recorded' in the set of functions $p_{k,t}(x)$, where $k$ runs over all the bond belonging to $\partial C_t$, while the last step is recorded in the particular functional relationship between $m_{i,t+1}(x)$ and the set $\{p_{k,t}(x)\}$ itself. This relationship is imposed by the order relation among the interface variable $x_k$, i.e. by the fact that $x_i$ is the minimum in $\partial C_t$. Note that, once a bond is broken, it no longer participates in the dynamics. For this reason, the 'effective' probability density function of its threshold no longer changes in time and is given definitely by equation (2).

For the remaining bonds one has to distinguish between the unbroken bonds far away from the bond $i$ and the unbroken nearest neighbour bonds, which will be weakened by the growth of bond $i$. The updating rules, for the two different mechanisms of damage, differ only for this last set of bonds. For the non-weakened bonds, one has in both cases the following updating equation:

$$p_{j,t+1}(x) = \frac{1}{\mu_{i,t}} p_{j,t}(x)\int_0^x \mathrm{d}y\; p_{i,t}(y)\left[\prod_{k(\neq i,j)}^{\partial C_t}\int_y^1 \mathrm{d}z\; p_{k,t}(z)\right]. \tag{3}$$

The updating equations for the weakened bonds are instead the following.

(1) For damage mechanism 1:

$$p_{j,t+1}(x) = \frac{1}{\mu_{i,t}}\int_0^1 \mathrm{d}y\,\frac{1}{y}\theta(y-x)p_{j,t}(y)\int_0^y \mathrm{d}z\; p_{i,t}(z)\left[\prod_{k(\neq i,j)}^{\partial C_t}\int_z^1 \mathrm{d}u\; p_{k,t}(u)\right]. \tag{4}$$

(2) For damage mechanism 2 (see the appendix):

$$p_{j,t+1}(x) = \frac{1}{\mu_{i,t}}\int_0^1 \mathrm{d}y\left[\prod_{k(\neq i,j)}^{\partial C_t}\int_y^1 \mathrm{d}z\; p_{k,t}(z)\right]p_{i,t}(y)p_{j,t}\left(x + \frac{y}{n_{i,t}}\right)$$
$$\times\theta\left(\frac{n_{i,t}}{n_{i,t}-1}x - y\right)\theta(n_{i,t}(1-x) - y). \tag{5}$$

Note that the main difference between equations (4) and (5) is due to the fact that the number of nearest neighbours $n_{i,t}$ of the bond $i$ at time $t$ appears explicitly only in the latter, i.e. only in the second model (rule 2) is the damage an explicit function of the geometry, while in the former (rule 1) the damage is a 'one-bond' process.

Equations (1)–(3) coincide with those introduced for the RTS approach to IP (apart from the different definition of the growth interface $\partial C_t$). Equations (4), (5), however, are new and account for the nearest neighbour weakening. Equations (1)–(5) allow one to study the extremal deterministic dynamics as a kind of stochastic process with memory. In particular, $\mu_{i,t}$ can be used to evaluate systematically the statistical weight of a fixed time-ordered growth path, while the $p_{j,t}(x)$ store information about the growth history.

A very important quantity to characterize the properties of the dynamics is the empirical distribution (or histogram) of unbroken thresholds. This quantity is defined as

$$h_t(x) = \sum_{j \in \partial C_t} p_{j,t}(x) \tag{6}$$

where $h_t(x)\,\mathrm{d}x$ is the number of non-broken bonds between $x$ and $x + \mathrm{d}x$ at time $t$, conditioned to the past dynamical history.

Considering the effect of the growth of bond $i$ at time $t$ on this quantity, one obtains

$$h_{t+1}(x) = h_t(x) - m_{i,t+1}(x) - \sum_{j(i)} p_{j,t}(x) + \sum_{j(i)} p_{j,t+1}(x) \tag{7}$$

where $j(i)$ indicates the sum over the $n_{i,t}$ unbroken nearest neighbours of $i$. Moreover, $m_{i,t+1}(x)$ and $p_{j,t+1}(x)$ are given respectively by equations (2)–(5) (for rule 2). Since the histogram is an almost self-averaging quantity of the model in the large-time limit, one can evaluate its shape in the 'typical' realization of the dynamics, taking the average over all the possible histories up to time $t + 1$. The notation $\langle \cdots \rangle$ is introduced to indicate this average. The lhs of equation (7) can be computed as

$$\langle h_{t+1}(x) \rangle = \|\partial C_{t+1}\| \phi_{t+1}(x) = [N - (t+1)]\phi_{t+1}(x) \tag{8}$$

where $N = 2L^2$ is the total number of bonds in the lattice and $\phi_t(x)$ represents the average threshold density function over the unbroken bonds at time $t$ (normalized to 1), i.e. $\phi_t(x) = p_{k,t}(x)$ where $k$ is a generic interface bond. For the rhs of equation (7) the main difficulty arises in the evaluation of $\langle m_{i,t+1} \rangle$ and $\langle \sum_{j(i)} p_{j,t+1}(x) \rangle$. Following [9], one can write

$$\langle m_{i,t+1} \rangle \simeq (N - t)\phi_t(x) \left[ 1 - \int_0^x \mathrm{d}y\, \phi_t(y) \right]^{N-t-1}. \tag{9}$$

In obtaining equation (9), we used the definition of $\phi_t(x)$ and the following approximation:

$$\left\langle \prod_{k \in \partial C_t} p_{k,t}(x_k) \right\rangle = \prod_{k \in \partial C_t} \langle p_{k,t}(x_k) \rangle = \prod_{k \in \partial C_t} \phi_t(x_k). \tag{10}$$

Using again the definition of $\phi_t(x)$, one obtains

$$\left\langle \sum_{j(i)} p_{j,t}(x) \right\rangle = n_t \phi_t(x) \tag{11}$$

where $n_t = \langle n_{i,t} \rangle$. Using equation (4), corresponding to the weakening rule 1, and the approximations given by equation (10), one has

$$\left\langle \sum_{j(i)} p_{j,t+1}(x) \right\rangle = \frac{n_t(N-t)}{N-t-1} \int_x^1 \mathrm{d}y\, \frac{\phi_t(y)}{y} \left\{ 1 - \left[ 1 - \int_0^y \mathrm{d}z\, \phi_t(z) \right]^{N-t-1} \right\}. \tag{12}$$

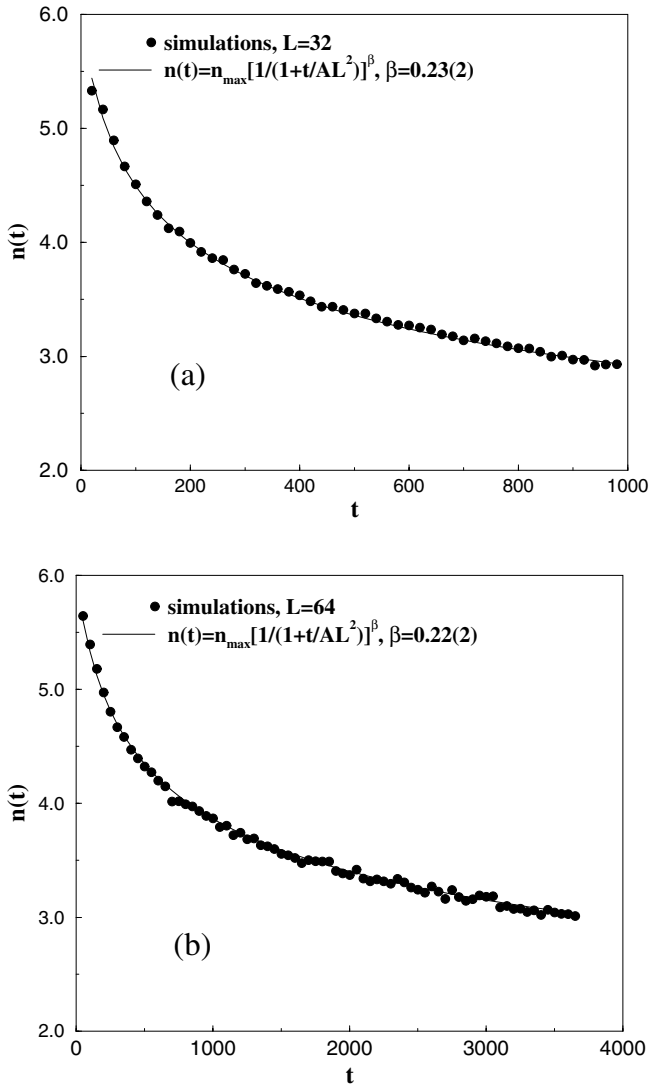


**Figure 2.** Fit of $n_t(L)$ with the scaling form (15) (weakening rule 1) for $L = 32$ (*a*) and 64 (*b*).

The equation for the $\phi_{t+1}(x)$ for rule 1 will finally read

$$\phi_{t+1}(x) = \frac{N-t-n_t}{N-t-1}\phi_t(x) - \frac{N-t}{N-t-1}\phi_t(x)\left[1-\int_0^x \mathrm{d}y\,\phi_t(y)\right]^{N-t-1} + n_t\frac{N-t}{(N-t-1)^2}\int_x^1 \mathrm{d}y\,\frac{\phi_t(y)}{y}\left\{1-\left[1-\int_0^y \mathrm{d}z\,\phi_t(z)\right]^{N-t-1}\right\}. \tag{13}$$

Note that even at percolation time $N - t$ is a large number. For this reason terms in equation (13) containing the term $[1 - \int_0^x \mathrm{d}y\,\phi_t(y)]^{N-t-1}$ are negligible for $x$ such that $\int_0^x \mathrm{d}y\,\phi_t(y)$ is finite (i.e. larger than $1/(N-t)$). It is easy to show that the continuum limit of equation (13), for such values of $x$, is invariant under the rescaling $L \to aL$ (i.e. $N \to a^2N$)

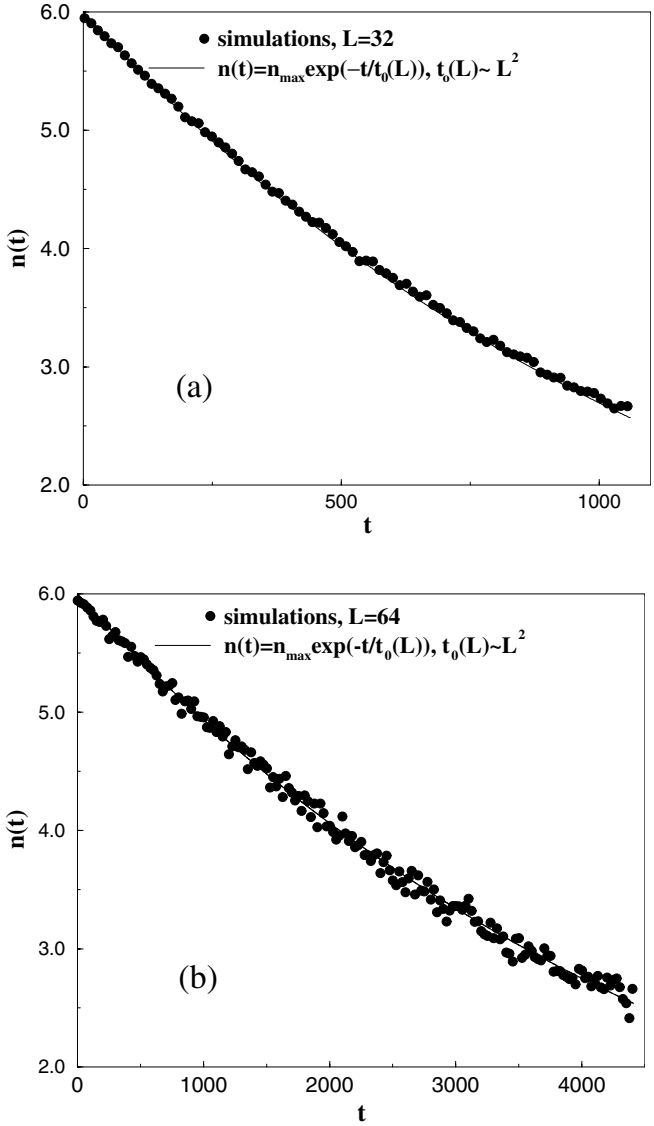


**Figure 3.** Fit of $n_t(L)$ with the scaling form (15) (weakening rule 2) for $L = 32$ (*a*) and 64 (*b*).

and $t \to a^2 t$. This result is based on the assumption that

$$n_t(L) = n_{a^2 t}(aL). \tag{14}$$

The numerical simulations suggest the following scaling form for $n_t(L)$ (see figure 2):

$$n_t(L) = n_{\max}\left[\frac{1}{1 + t/AL^2}\right]^{\beta} \tag{15}$$

where $\beta = 0.23(2)$, $A = 0.030(2)$ and $n_{\max} = 6$ is the lattice coordination number. This form for $n_t$ satisfies equation (14).

The study of weakening rule 2 is quite similar. Equations (1)–(3) remain the same, while the conditioned probability density for the weakened bonds is given by equation (5).

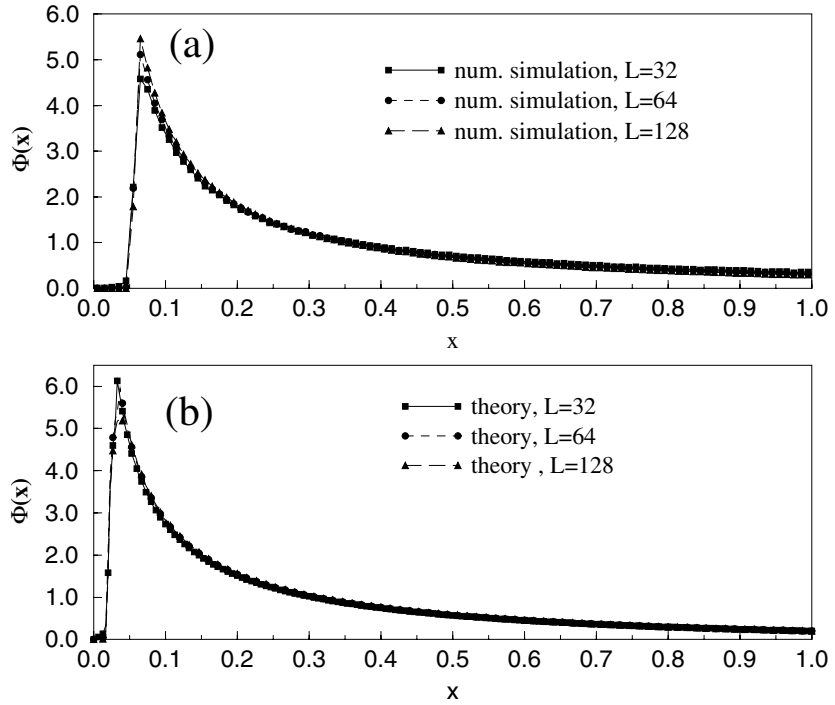


**Figure 4.** Solution of equation (13) for the histogram $\phi_t(x)$ at the spanning time ($b$), compared with simulations ($a$), for weakening rule 1.

By following the same steps as above, the following equation for $\phi_{t+1}(x)$ is obtained:

$$\phi_{t+1}(x) = \frac{N-t-n_t}{N-t-1}\phi_t(x) - \frac{N-t}{N-t-1}\phi_t(x)\left[1-\int_0^x \mathrm{d}y\,\phi_t(y)\right]^{N-t-1}$$
$$+n_t\frac{N-t}{N-t-1}\int_0^1 \mathrm{d}y\left[1-\int_0^y \mathrm{d}z\,\phi_t(z)\right]^{N-t-2}\phi_t(y)$$
$$\times\phi_t\left(x+\frac{y}{n_t}\right)\theta\left(\frac{n_t}{n_t-1}x-y\right)\theta(n_t(1-x)-y). \tag{16}$$

All the assumptions we made for case 1, including the scaling ansatz given in equation (14), are valid for case 2. In particular, from numerical simulations, one can find the following behaviour for $n_t(L)$ (see figure 3):

$$n_t(L) \simeq n_{\max}\exp\left(-\frac{t}{AL^2}\right). \tag{17}$$

The analytical study of both kinds of weakening allows us to make three important predictions. First, we find both theoretically, from the numerical solution of equations (13), (16), and from the numerical simulations of the model, a discontinuity in the histogram (see figures 4 and 5), indicating that the system evolves in such a way as to remove all bonds with threshold smaller than some critical value $x_c$. Second, from the symmetry properties of equations (13), (16), we deduce that the number $t_{sp}(L)$ of broken bonds at the percolation time is proportional to $L^2$, even though the percolating cluster is fractal. This result, confirmed by numerical simulations (see figures 6($a$) and 7($a$)), and compatible with the scaling function (15) for $n_t(L)$, is deduced supposing that at the percolation time the shape of the histogram is independent of $L$, an

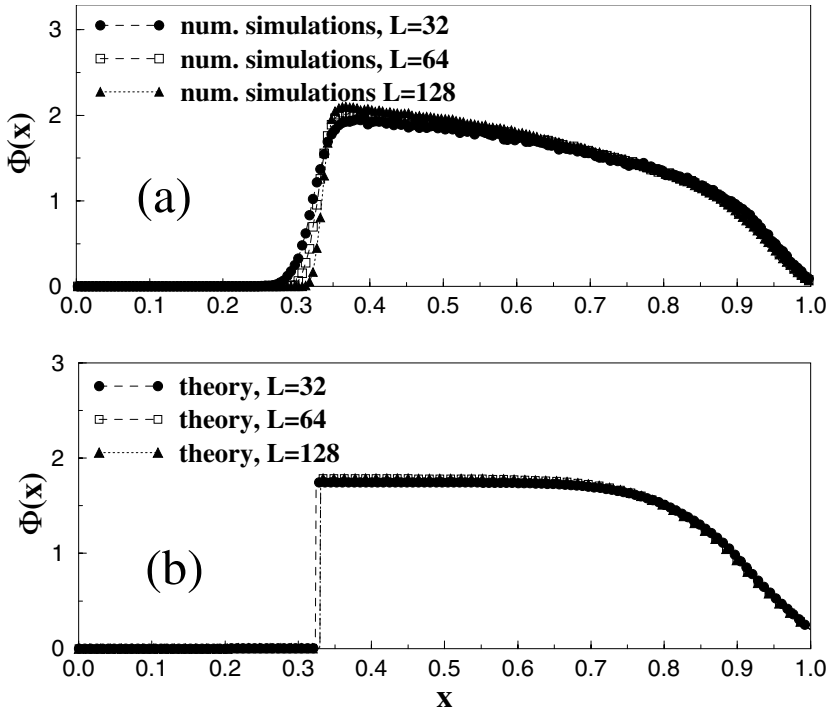


**Figure 5.** Solution of equation (13) for the histogram $\phi_t(x)$ at the spanning time ($b$), compared with simulations ($a$), for weakening rule 2.

assumption which fits well with the numerical histogram (see figures 4($a$) and 5($a$)). Finally, we present an approximated result for the dynamical behaviour of the average value (over the unbroken bonds) of the thresholds $\langle x\rangle(t)$. This quantity can be seen as a characterization of the average resistance of the material in time.

In order to find the evolution equation of $\langle x\rangle(t)$ for damage rule 1, it is enough to multiply both sides of equations (13) and (16) by $x$ and integrate them in the whole interval [0, 1]. Then one finds

$$\langle x\rangle(t+1) = \left(1 - \frac{n_t - 2}{2(N-t-1)}\right)\langle x\rangle(t) - \frac{1 + n_t/[2(N-t-1)]}{N-t-1}\int_0^1 \mathrm{d}x\left[1 - \int_0^x \mathrm{d}y\,\phi_t(y)\right]^{N-t}. \tag{18}$$

For damage rule 2, the way to find the equation for $\langle x\rangle$ is even simpler. In fact, it is enough to consider that at each time-step, the global effect on $\langle x\rangle$ is equivalent to removing two bonds with resistance equal to the minimal one at that time. Therefore, one can write

$$\langle x\rangle(t+1) = \left(1 + \frac{1}{N-t-1}\right)\langle x\rangle(t) - \frac{2}{N-t-1}\int_0^1 \mathrm{d}x\left[1 - \int_0^x \mathrm{d}y\,\phi_t(y)\right]^{N-t}. \tag{19}$$

For rule 1, it is simple to see, from equation (18), that $\langle x\rangle(t+1) < \langle x\rangle(t)$ until $n_t > 2$ (which is verified for all times). This means that on average the medium weakens during the evolution even if the weakest bond is removed at any time step. This is due to the fact that, in this case, the weakening of the neighbours of the weakest interface bond has a stronger effect on the material than the removal of the weakest bond itself. For rule 2, instead, one finds that

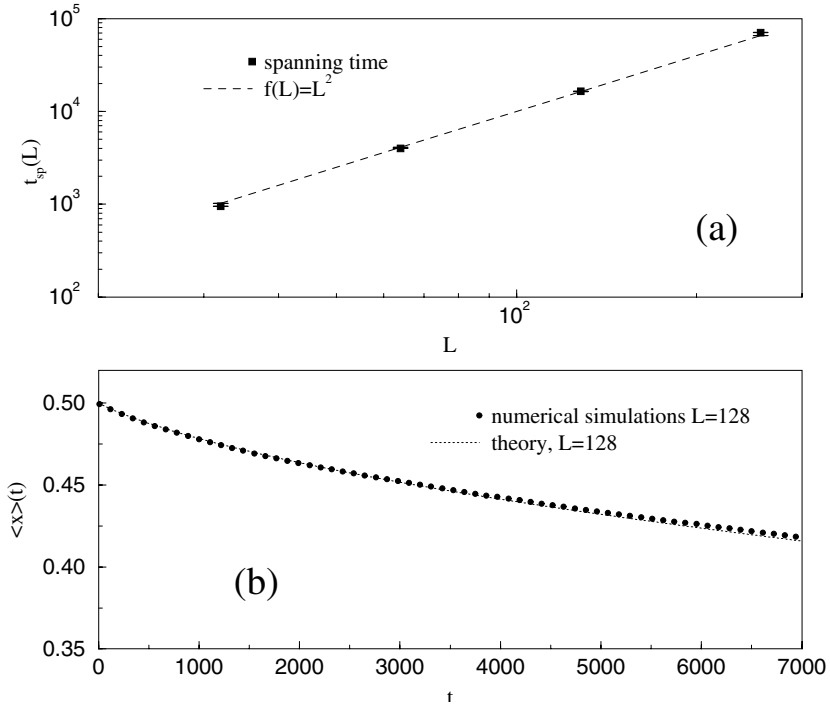


**Figure 6.** (*a*) Spanning time versus system size $L$ for weakening rule 1. One can see a good agreement with the expected scaling law $t_{\rm sp}(L) \propto L^2$. (*b*) Solution of equation (18) compared with numerical simulations.

$\langle x\rangle(t+1) > \langle x\rangle(t)$, if $\langle x\rangle(t)$ is larger than twice the average minimal threshold, and, due to the extremal nature of the dynamics, this is verified always in the large-$N$ limit, i.e. in the limit of a large number of bonds in the interface at any time-step. This means that, in this second case, the damage is not strong enough to allow a global weakening of the system, which becomes more and more rigid. This is reasonable since in rule 2 the stress on the weakest bond is redistributed to the nearest neighbour and the total initial stress is conserved, while in rule 1 there is no total stress conservation. In other words, in the model with rule 1 the damage is a multiplicative effect, i.e. the damage is proportional to the old threshold (which can be big); in the model with rule 2 the damage is reduced by the fact that at each time-step it is proportional to the minimal threshold in the whole system. In figures 6(*b*) and 7(*b*) the time evolution of $\langle x\rangle(t)$ obtained from computer simulations is compared with the theoretical prediction. Our analytical results are in good agreement with numerical simulations. For rule 2, numerical simulations of the histogram show a low-$x$ tail below the critical threshold, which tends to disappear as the system size grows, and a non-zero slope of the part just above the critical threshold. The first one is clearly a finite-size effect, which plays a minor role in the simulations with rule 1, because for rule 1 the critical threshold is very small. Of course, such a finite-size effect is absent from the theoretical results, as in all mean-field (MF) approaches. The second effect could be due to spatial correlation induced by damage rule 2, which in the analytical approach are neglected. This second effect does not disappear as the system size grows. Consequently the agreement between the numerical simulations of $\langle x\rangle(t)$ and equation (19) is less good than for rule 1. The numerical $\langle x\rangle(t)$, mainly because of the non-zero negative slope of $\phi(x)$ above $x_{\rm c}$, is a little smaller than the theoretical prediction.

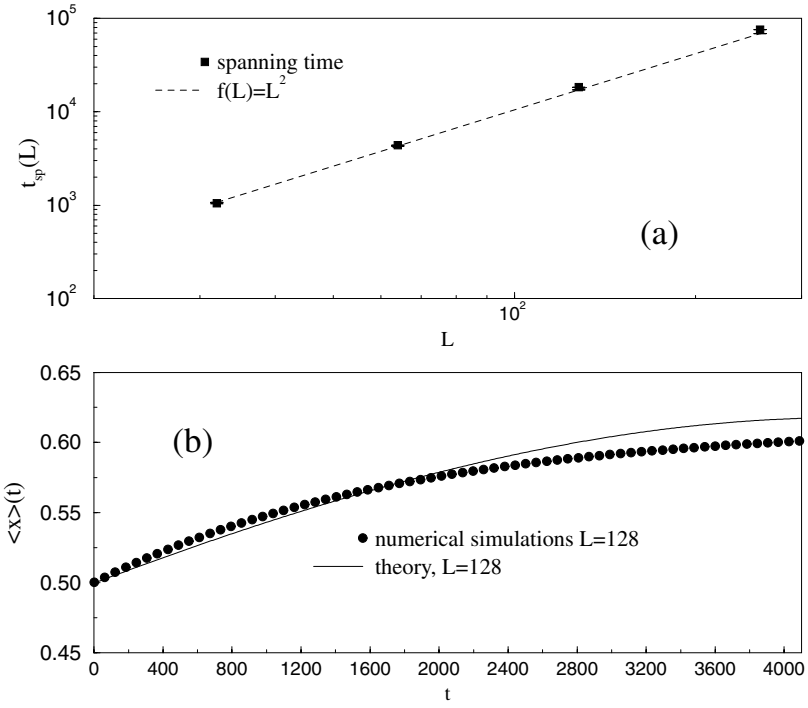


**Figure 7.** (*a*) Spanning time versus system size $L$ for weakening 2. In this case also, there is very good agreement with the expected scaling law $t_{\mathrm{sp}}(L) \propto L^2$. (*b*) Solution of equation (19) compared with numerical simulations.

With respect to real fracturing processes the behaviour of the average resistance $\langle x \rangle(t)$ obtained with rule 2 is more realistic, since in real materials one usually observes that the material during micro-crack formation becomes more rigid, although more fragile, since the number of bonds one has to break to have global breakdown becomes smaller and smaller. Moreover it is worth noting that, apart from the shape of $\phi(x)$ and the behaviour of $\langle x \rangle(t)$, none of the statistical properties of the system depend on the weakening rule used.

Finally, it is worthwhile to point out that, to our knowledge, apart from the qualitative results of [5], no quantitative experimental results are available. For example, a measurement of the fractal dimension of cracks or their size distribution would be extremely useful to further test the predictions of this model. At the moment, this model seems able to capture, with its extremely simplified dynamics, some basic properties of fracturing processes for thin layers of material under desiccation.

In conclusion, we have presented a new model for fractures, which is useful in describing in a semi-quantitative way some basic mechanisms in drying paint- and mudlike cracking processes, for extremely thin samples. Due to its extreme simplicity, the model is particularly suitable for large-scale simulations and takes into account the damage effects involved in fracture propagation. Even in this simple model we are able to analyse which conditions trigger SOC behaviour in such systems. Furthermore, the change in the threshold distribution, induced by the damage mechanism, allows us to write down explicitly the form of the breakdown probability for the bonds of the sample. Possible further research could include, for damage rule 2, a more refined computation scheme, in which two variable probability densities are

also considered. This would be the first-order correction to our MF approach considering only one-variable distributions, and could allow us to take into account correlations induced by the damage rule. Such a generalization of the RTS theory, formally discussed in [19], is however very difficult technically. Another possible extension of this paper we are considering now is to apply real space renormalization group techniques, combined with the RTS approach, to calculate the critical exponents of the model.

**Acknowledgment**

The authors acknowledge the support of the EU grant contract no FMRXCT980183.

## Appendix. RTS for the damaged system

In this appendix we provide a simple derivation of the RTS probabilistic equations. As a general remark, one has to note that in this kind of model (as well as in IP) the initial condition of the system is characterized by independent variables (the breaking thresholds of the bonds), identically and uniformly distributed. However, once the minimal value in the set is found and the relative bond broken, the knowledge of this event makes the variables of the remaining non-broken bonds no longer simply uniformly distributed in the interval [0, 1], and correlated (no longer independent of one other). In fact, after the breaking of the bond with the minimal threshold, one has to *condition* the probability of any further event to the last known event. This information influences the probability distribution of the remaining bonds of the system and creates correlations among them [21].

The systematic study of this 'memory' effect is what is called RTS [9, 19].

In order to clarify the 'step by step' mechanism of storage of conditional information, let us consider a fixed time-order path $A_t$, i.e. a *history* of the dynamics up to time $t$. $A_t$ is given by the time ordered sequence $\{i_0, i_2, \ldots, i_{t-1}\}$ of the broken bonds up to time $t$. Let us suppose we know the joint threshold probability density function $P_t(\{x\}_{\partial C_t}|A_t)$ of the whole set of non-broken bonds conditioned to the knowledge of the past history $A_t$. $P_t(\{x\}_{\partial C_t}|A_t)$ represents the 'effective' distribution of the disorder at the $t$th time-step of a fixed history $A_t$. Note that at time $t = 0$, one has

$$P_0(\{x\}_{\partial C_0}) = \prod_{k\in S} p_0(x_k) = 1 \tag{A1}$$

where $S$ is the whole lattice, as no information from the dynamics is still present.

Since any kind of 'order' relation, superimposed on a set of independent stochastic variables, introduces correlations, in general $P_t(\{x\}_{\partial C_t}|A_t)$ does not factorize in the product of single-bond 'effective' density functions for $t > 0$ [21]. That is, it is not possible to write

$$P_t(\{x\}_{\partial C_t}|A_t) = \prod_{k\in\partial C_t} p_{k,t}(x_k). \tag{A2}$$

However, as shown in [20], in the limit of large number of variables the 'geometrical' correlations in $P_t(\{x\}_{\partial C_t}|A_t)$ become negligible, and one can make, at any time-step, the approximation given by equation (A2). Therefore, we consider the approximated case where the 'effective' probability density function of the disorder of the system, with all the information about the past history stored, is given by the set of 'effective' one-bond functions $p_{k,t}(x)$ for each non-broken bond $k$. The rigorous exposition of RTS, by using the non-factorizable function $P_t(\{x\}_{\partial C_t}|A_t)$ at each $t$ is given in [19].

Knowing the set of functions $p_{k,t}(x)$, one can write the 'effective' probability $\mu_{i,t}$ that a given bond $i$ of the set is broken at that time. It is simply the probability, conditioned

to the whole past history, that $x_i$ is the minimum in the set of non-broken bond variables. Consequently, it is given by equation (1), i.e.

$$\mu_{i,t} = \int_0^1 \mathrm{d}x\; p_{i,t}(x)\left[\prod_{k(\neq i)}^{\partial C_t} \int_x^1 \mathrm{d}y\; p_{k,t}(y)\right]. \tag{A3}$$

The set of $\mu_{i,t}$, for each non-broken bond and for each time-step, defines a branching process of the dynamics; i.e. each history $A_t$ at time $t$ continues with a certain probability $\mu_{i,t}$ in a different history $A_{t+1}$ at time $t+1$ for each breaking bond $i$ at time $t$. In order to continue the probabilistic description of the branching at further time-steps, one should obtain the new set of functions $p_{k,t+1}(x)$ for these different cases of breaking at time $t$, using only the 'old' set of $p_{k,t}(x)$ and the set of probabilities $\mu_{i,t}$ defining the branching. This is possible by using the notions of conditional probability. Here the simple rule relating the conditional to joint probability of a first event $A$ to a second event $B$ is recalled [21]:

$$\mathrm{Prob}(A|B) = \frac{\mathrm{Prob}(A \cap B)}{\mathrm{Prob}(B)} \tag{A4}$$

where, as usual, $A|B$ means the event $A$ *conditioned* to the event $B$, while $A \cap B$ the event $A$ *joint* to the event $B$.

Note that 'memory' up to time $t$, for a fixed history $A_t$ in the branching of all the possible histories, is already stored in the functions $p_{k,t}(x)$. Consequently, in order to obtain the set of probability functions $p_{k,t+1}(x)$ for the history $A_{t+1}$ obtained from $A_t$ adding the breaking of bond $i$ at time $t$, one has to store only information about the last step.

At this point one has to distinguish the three cases: (1) the just broken bond $i$, (2) a non-broken bond $j$ far from $i$ and (3) a non-broken neighbour $l$ of $i$.

In case (1) let us call the conditioned probability density of bond $i$ after its breaking $m_{i,t+1}(x)$ instead of $p_{i,t+1}(x)$, remarking with this that after its breakdown, bond $i$ is removed definitely from the interface. Note that, since after $t$ the bond $i$ does not participate in the dynamics, its 'effective' probability density will no longer change. $m_{i,t}(x)\,\mathrm{d}x$ is the probability that $x < x_i \leqslant x + \mathrm{d}x$, conditioned to the the past history up to its breaking. However, since the memory up to the time-step just before its breaking is stored in the known functions $p_{k,t}(x)$, $m_{i,t}(x)\,\mathrm{d}x$ is the probability, calculated using the set of functions $\{p_{k,t}(x)\}$, that $x < x_i \leqslant x+\mathrm{d}x$ (event $A$ of equation (A4)) conditioned to the fact that the bond $x_i$ is the minimum in the set of interface bonds at that time (event $B$ of equation (A4)). Therefore, from equation (A4), one has equation (2):

$$m_{i,t+1}(x) = \frac{1}{\mu_{i,t}} p_{i,t}(x)\left[\prod_{k(\neq i)}^{\partial C_t} \int_x^1 \mathrm{d}y\; p_{k,t}(y)\right]. \tag{A5}$$

In a quite similar way we can update the effective probability densities for cases (2) and (3). In case (2), using the set of functions $\{p_{k,t}(x)\}$, $p_{j,t+1}(x)\,\mathrm{d}x$ is the probability that $x < x_j \leqslant x+\mathrm{d}x$ (event $A$) conditioned to the fact that $x_i$ was the minimal value in the interface at time $t$. Again from equation (A4) one has equation (3):

$$p_{j,t+1}(x) = \frac{1}{\mu_{i,t}} p_{j,t}(x) \int_0^x \mathrm{d}y\; p_{i,t}(y)\left[\prod_{k(\neq i,j)}^{\partial C_t} \int_y^1 \mathrm{d}z\; p_{k,t}(z)\right]. \tag{A6}$$

In case (3) one has to distinguish the two different damage rules, and the conditioning events are more complex. For rule 1, using the set of function $\{p_{k,t}(x)\}$, $p_{l,t+1}(x)\,\mathrm{d}x$ is the probability that $x < x_l \leqslant x + \mathrm{d}x$ (event $A$) conditioned to the fact that $x_i$ was the minimum and that

the value of $x_l$ at this time-step differs from the value at the previous time-step for a random fraction of itself (event $B$). One, then, obtains equation (4):

$$p_{j,t+1}(x) = \frac{1}{\mu_{i,t}} \int_0^1 \mathrm{d}y \, \frac{1}{y} \theta(y - x) p_{j,t}(y) \int_0^y \mathrm{d}z \; p_{i,t}(z) \left[ \prod_{k(\neq i,j)}^{\partial C_t} \int_z^1 \mathrm{d}u \; p_{k,t}(u) \right]. \tag{A7}$$

Finally, for rule 2, always using the set of functions $\{p_{k,t}(x)\}$, $p_{l,t+1}(x)\,\mathrm{d}x$ is the probability that $x < x_l \leqslant x + \mathrm{d}x$ (event $A$) conditioned to the fact that $x_i$ was the minimum and that the value of $x_l$ at this time-step differs from the value at the previous time-step for a fraction $1/n_{i,t}$ of $x_i$ (event $B$). From this one has equation (5)

$$p_{j,t+1}(x) = \frac{1}{\mu_{i,t}} \int_0^1 \mathrm{d}y \left[ \prod_{k(\neq i,j)}^{\partial C_t} \int_y^1 \mathrm{d}z \; p_{k,t}(z) \right] p_{i,t}(y) p_{j,t} \left( x + \frac{y}{n_{i,t}} \right)$$
$$\times \theta \left( \frac{n_{i,t}}{n_{i,t} - 1} x - y \right) \theta(n_{i,t}(1 - x) - y). \tag{A8}$$

## References


[1] Herrmann H J and Roux S (ed) 1990 *Statistical Models for the Fractures of Disordered Media* (Amsterdam: North-Holland)
[2] Sahimi M 1998 *Phys. Rep.* **306** 213
[3] Chackrabarti B K and Benguigni L G 1997 *Statistical Physics of Fracture and Breakdown in Disordered Systems* (Oxford: Oxford University Press)
[4] Gabrielli A, Cafiero R and Caldarelli G 1990 and 1999 *Europhys. Lett.* **45** 13
[5] Groisman A and Kaplan E 1994 *Europhys. Lett.* **25** 415
[6] Wilkinson D and Willemsen J F 1983 *J. Phys. A: Math. Gen.* **16** 3365
[7] Caldarelli G, Castellano C and Vespignani A 1994 *Phys. Rev.* E **49** 2673
Caldarelli G, Di Tolla F D and Petri A 1996 *Phys. Rev. Lett.* **77** 2503
[8] Zapperi S, Vespignani A and Stanley H E 1997 *Nature* **388** 658
[9] Marsili M 1994 *J. Stat. Phys.* **77** 773
Gabrielli A, Cafiero R, Marsili M and Pietronero L 1997 *Europhys. Lett.* **38** 491
[10] Sornette D and Vanneste C 1991 *Phys. Rev. Lett.* **68** 612
[11] Carol I and Bazant Z P 1993 *J. Eng. MECH-ASCE 119* 2252–69
[12] Neal J T 1966 *Geol. Soc. Am. Bull.* **76** 1075
Neal J T and Motts W S 1967 *J. Geol.* **75** 511
Korvin G 1989 *Pure. Appl. Geophys.* **131** 289
[13] Walker J 1986 *Sci. Am.* **255** 178
[14] Wittmann F H, Slowik A and Alvaredo A M 1994 *Mater. Struct.* **27** 499
Nishikawa T and Takatsu M 1995 *Cement Concrete Res.* **25** 1218
[15] Hoshen J and Kopelman R 1976 *Phys. Rev.* B **14** 2428
[16] Petri A, Paparo G, Vespignani A, Alippi A and Costantini M 1994 *Phys. Rev. Lett.* **73** 3423
[17] Bak P, Tang C and Wiesenfeld K 1987 *Phys. Rev. Lett.* **59** 381
[18] Bak P and Sneppen K 1993 *Phys. Rev. Lett.* **71** 4083
[19] Gabrielli A 2000 Memory effects in stochastic growth dynamics with quenched disorder: the generalized run time statistics, in preparation
[20] Cafiero R, Gabrielli A and Marsili M 1997 *Phys. Rev.* E **55** 7745
[21] Feller W 1965 *An Introduction to Probability Theory and its Applications* vol 1 and 2 (New York: Wiley)